A NUMERICAL-EXPERIMENTAL APPROACH TO MATERIAL CHARACTERIZATION AND PROCESS ANALYSIS IN THE BLOW FORMING PROCESS

D. Sorgente, L. Tricarico

A NUMERICAL-EXPERIMENTAL APPROACH TO MATERIAL CHARACTERIZATION AND PROCESS ANALYSIS IN THE BLOW FORMING PROCESS

Donato SORGENTE [1], Luigi TRICARICO [1]

[1] Dipartimento di Ingegneria Meccanica e Gestionale, Politecnico di Bari – Viale Japigia, 182 – 70124 BARI - ITALY
d.sorgente@poliba.it, tricarico@poliba.it

Abstract

In carrying out a superplastic forming process, the first step for the process optimization is a detailed material characterization. The achievement of a successfully formed component is strictly related to the material behaviour: commonly, several tensile tests are carried out at different temperatures and strain rates for locating the best deformation parameters, corresponding to which maximum uniform elongation of the material can be found. Additionally, characterization is needed also for estimating material parameters to numerically model the process. Numerical modelling is a necessary step when the pressure profile of a blow forming process has to be optimized. In this paper authors present a methodology for estimating material parameters on the basis of few bulge tests and for analysing the superplastic forming process. Temperature and pressure influences are analysed by means of free inflation tests. Material parameters are calculated starting from an analytical approach and refining the solution by an inverse analysis. A 3D numerical model of the process has been then created and used for evaluating the pressure profile that is able to keep the strain rate value in the sheet close to a target value. A numerical-experimental comparison has been done for testing the model capability and effectiveness of the pressure profile in a prismatic closed die blow forming test. Good agreement has been found between experimental results and numerical simulations. Thickness distribution measurements, optical microscope observations, post-forming characteristics evaluation have been performed to compare constant pressure and constant strain rate tests.

Keywords:
Superplasticity; material characterization; blow forming.

1 INTRODUCTION

In the superplastic (SP) field, the individuation of the appropriate forming temperature and strain rate is the first step for a successful process implementation but also for its optimization. Usually to understand the best process parameters, tensile tests are carried out on several specimens at different temperatures and strain rates. The temperature and the strain rate that lead to the highest uniform elongation, corresponding to the higher strain rate sensitivity index *m*, are considered as process parameters for the following step. The superplastic forming (SPF) process is then performed on the basis of tensile tests results. In spite of the consolidated interest in SP light metallic alloys, it is not so simple to find information in the specific literature, because every kind of treatment brings to different material characteristics and, even if the alloy composition of two samples and their mean grain size are similar, their behaviour could be very different as far as SPF applications are concerned [1]. Furthermore, since Finite Element (FE) numerical modelling and analysis have gained great potentialities and interest in the simulation of forming processes, material characterization and constitutive modelling have become of great significance not only for predicting material behaviour but also for directly optimizing process parameters. Many constitutive equations have been studied and verified for describing and modelling the behaviour of SP materials [2]. In a blow forming (BF) process, the optimal strain rate can be achieved and kept constant on the sheet changing the gas pressure value according to a specific law. This kind of law is generally created by a numerical FE model in order to keep the strain rate constant and close to the optimal value in the whole sheet. Thus, the quality of the formed part is strongly influenced by the accurateness of material constants used in the FE model. Last studies are focused also in obtaining very accurate pressure laws where the equivalent target strain rate is managed and varied during the process for enhancing material properties taking into account also microcavities evolution and grain growth effects [3]. In

this case material constants become further important as the constitutive equation must consider also parameters like static and dynamic grain growth and cavity growth. Other efforts have been also made in analysing possible differences between the uni-axial characterization by tensile tests and other alternative method with strain conditions more similar to the forming process ones [4,5].
Post-forming mechanical strength of the material is a very important matter in SPF applications: as material goes under cavitation and grain growth, the mechanical strength after forming can be seriously affected according to the forming parameters. Since each geometry and each particular application have different strength requirements, there are not specific procedures to characterize the formed material, but several studies can be found in literature where tensile test specimens have been machined from the formed component and tested to evaluate post-forming static and dynamic strength [6,7].
In this work authors have analyzed the SP behaviour of a superplastic aluminium AA7475 alloy. Blanks with an initial thickness of 0.8 mm have been used in the whole experimentation. The SP behaviour of this material has been considered well approximated by the Backofen equation where the equivalent stress is related to the equivalent strain rate by a power law. The characterization has been done with preliminary free inflation constant pressure tests at different temperature and pressure values. Material constants have been calculated by an analytical approach and then verified with a simple 2D FE numerical model. An inverse technique with a gradient-based method has been then used to calibrate the material behaviour in the FE model. Closed die BF tests have been then carried out in a prismatic die cavity, with constant pressure and different forming times. A 3D model of these tests have been created and the pressure profile able to keep the strain rate along the sheet constant have been estimated. Then constant strain rate pressure law has been applied on the sheet in experimental tests. The formed specimen obtained with that pressure profile has been compared, in terms of thickness distribution, microcavities and post-forming tensile strength, with the specimen obtained with constant pressure.

2 EXPERIMENTAL FACILITY

Both the material characterization and the closed die forming tests have been performed on a laboratory scale Blow Forming (BF) equipment embedded in the cylindrical split furnace of an INSTRON universal testing machine (max load 200kN). The equipment consists in: (i) a blank-holder, (ii) female dies with different cavity shapes for generating on the blank different forming conditions, (iii) a pneumatic circuit for the gas supply with an Argon (Purity: 99.990%) cylinder, proportional electronic valves, steel tubes in the proximity of the forming chamber and flexible polyurethane tubes in colder zones, (iv) an electrical furnace (max power 3kW, precision ± 2°C) with its electronic controllers for upper, central and lower zones which can be set with three different temperatures for compensating thermal dispersion, (v) thermocouples to monitor thermal condition on the sheet and on the tools, (vi) a transducer for measuring, during free inflation test, the dome height on the specimen and (vii) a PC with a data acquisition I/O device by which gas pressure, temperature, blankholder force can be monitored and managed. A little fan, just out of the furnace, is used for the cooling of the upper part of the equipment to avoid excessive heating near the load cell of the INSTRON machine. In this equipment the undeformed sheet is interposed between the creep-resistant steel tools (the die and the blankholder) and the gas pressure acts on one side of the sheet forcing it to copy the geometry of the die cavity. Since forming tools are embedded in the split furnace of the INSTRON machine, the die and blankholder dimensions have been designed to fit the internal furnace diameter (90mm). A blankholder force, which allows having no drawing during the test and no gas leakages from the forming chamber, is applied before the gas adduction and kept constant during the whole test. For material characterization, bulge tests are performed with a cylindrical die cavity (inner diameter 45 mm) in which the sheet can freely expand; the dome height of the specimen is monitored

during the whole test by the digital acquisition of the position transducer signal. It is not worthless to notice that the specimen cutting accurateness is much less relevant than in traditional tensile tests where the gauge length zone has to be precisely finished to avoid crack propagation during the test. Further details about the equipment can be found in [8].
Using the same equipment described above and a die with a different cavity shape, closed die tests can be performed and the real forming process can be analysed in a more detailed way. Since some of the most common limits of forming technologies are the minimum corner radius that the sheet can fill without ruptures and the non axially symmetric filling of the die cavity, a prismatic die cavity was chosen for testing the material and the process capabilities in closed die forming tests. A die with a 14.5mm deep prismatic cavity has been used. The cavity has a squared section with a side length of 40 mm and a fillet radius between sides of 5 mm.

3 MATERIAL CHARACTERIZATION

Material characterization has been based on few free inflation tests performed on the aforementioned BF equipment. As summarized in the schematic flow chart in Fig. 1, material constants have been found first by an analytical approach and then, after the creation of a 2D numerical model of the free inflation test, by optimizing their values by an inverse analysis.

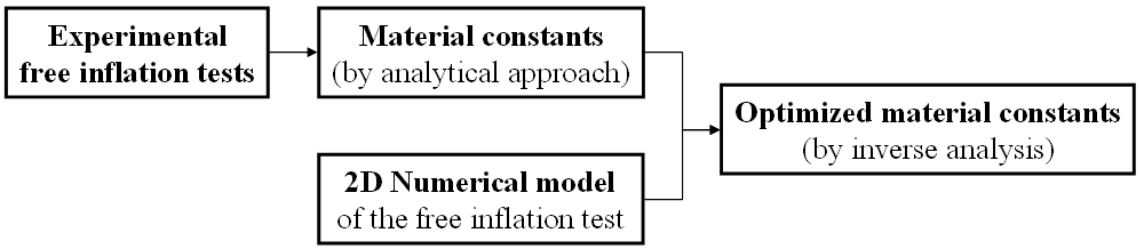

Figure 1. Schematic flow chart of the material characterization phase.

3.1 FREE INFLATION TESTS

The cylindrical cavity in the female die in which the sheet expands, is depth enough to carry on the test till the failure of the material without any contact between the sheet and the die bottom. In the experimental plan two levels of temperature (410°C and 460°C) and two levels of pressure (0.3 MPa and 0.7 MPa) has been used for testing material formability, as shown in Fig. 2.

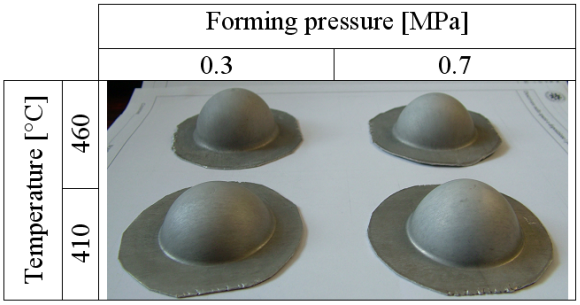

Figure 2. Material characterization: scheme of the experimental plan and corresponding specimens.

All the specimens tested in the experimental plan have failed on the dome apex, except for the test carried out with the lowest pressure and temperature levels, in which, after 5000 s, gas pressure was stopped even if the failure of the material was not achieved. Best formability was observed for the lowest pressure level on the highest temperature (0.3 MPa at 460°C) were the specimen reached a final dome height of 25.9 mm that corresponds to a normalized

polar height (dome height to die inner radius ratio) of 1.15. In the explored range, the highest temperature level appears to be the most suitable for obtaining SP deformation on the examined material.
In Fig. 3 the dome height evolution is shown for all the tests carried out for the material characterization. Pressure and temperature have similar effect on the strain rate imposed on the sheet: increasing either pressure or temperature brings to a reduction of the forming time that the sheet needs to get to a fixed height.

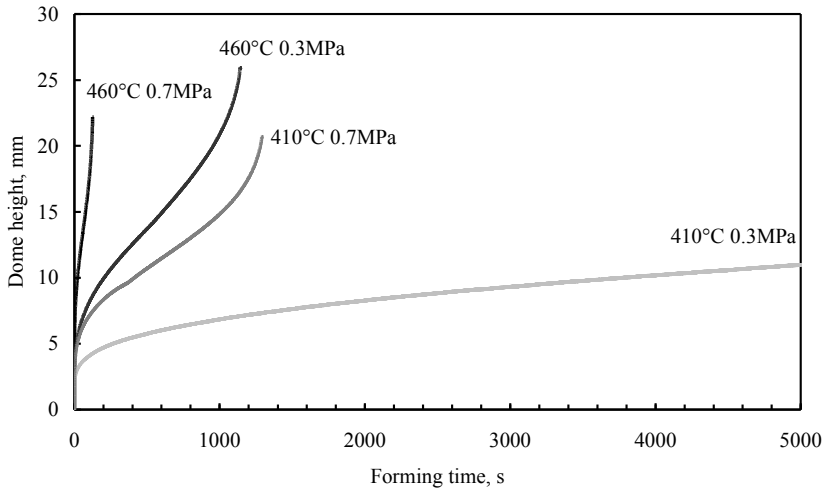

Figure 3. Material Characterization: dome height evolution of free inflation tests.

In order to develop and to verify the proposed characterization methodology and to analyze the process potentialities, a single temperature level (460°C) was chosen and considered in the following numerical and experimental BF tests.

3.2 Analytical approach

According to one of the first analytical approaches that has been followed by Jovane (1968), during a bulge test of a thin SP sheet in a cylindrical die, some assumptions can be done: the material is isotropic, the volume remains constant, elastic strains are negligible, the thickness to diameter ratio of the sheet is very small and bending effects are negligible, at any instant the sheet is equivalent to part of a thin sphere subjected to internal pressure, so that the curvature and the thickness are uniform and a state of uniform biaxial tension exists at any point on the sheet [9]. Starting from these assumptions many researcher has built up models of the BF of thin sheet; among them, Cheng developed a method for the evaluation of material parameters from a simple inflation test done with a BF equipment with a constant forming pressure; Enikeev and Kruglov, starting from two bulge tests with two different pressure values, proposed a method to obtain material constants and to take into account the non-uniform thickness distribution along the sheet [5,10].
In this work, for the chosen temperature level and starting from the following equation:

$$\sigma = C \cdot \dot{\varepsilon}^{m} \tag{1}$$

where σ is the equivalent stress, $\dot{\varepsilon}$ is the equivalent strain rate, C, the strength coefficient, and m, the strain rate sensitivity index, material constants have been calculated by the method proposed by Enikeev and Kruglov, considering free inflation tests obtained, at 460°C, at two different pressure levels (0.3 MPa and 0.7 MPa).

3.3 2D numerical model of free inflation test

A simple axially symmetric numerical model has been created using the commercial FE code ABAQUS with an elasto-viscoplastic integration. The deformable part corresponding to the aluminium blank has been divided into continuum elements with 4 nodes and one integration point, the die and the blankholder have been considered perfectly rigid. The sheet has been constrained in its periphery to have no translations and allowing only changing its thickness. The temperature has been considered perfectly stable and the material has been modelled with Eq. 1. In the ABAQUS software, for viscoplastic material, the CREEP option is available and the equivalent creep strain in the elements is computed by a power law of the equivalent deviatoric stress:

$$\Delta\varepsilon = \dot{\varepsilon}\cdot\Delta t = A\cdot\sigma^{n}\cdot\Delta t \tag{2}$$

where Δt is the time increment in the implicit integration and material constants can easily be related to the Eq. 1 ones: $A=(1/C)^{1/m}$ and $n=1/m$ [11].

3.4 Inverse analysis

To understand if the calculated values of C and m are sufficiently accurate in predicting material behaviour, they have been directly input in the numerical model. Experimental conditions have been simulated for the free inflation tests described in section 3.1. The numerical height evolution during the inflation tests has been compared with the experimental one and the error between numerical and experimental results has been quantified by an objective function Q: the smaller this function the sharper the numerical result. This function is based on information not only related to the final strain distribution of the specimen, but, since hot forming applications are strongly affected by time and strain rate, this function is build also on time evolution of the deformed shape of the specimen. Therefore, to distinguish good solutions from bad ones, the time evolution of the dome height has been taken into account. The dome height h curve has been approximated with a six order polynomial equation. The Q function is computed as follows:

$$Q=\frac{\sum_{i=1}^{N} Q_i}{N} \quad \text{with} \quad Q_i=\left[\frac{h_{comp}(t_i)-h_{\exp}(t_i)}{h_{\exp}(t_i)}\right]^2 \tag{3}$$

where the subscript *comp* indicates the computed values (from the FE simulation), *exp* the experimental ones, t_i are time values of the N numerical frames at which the computation is done (it depends on the output file of the simulation).
The minimum seek of the Q function is done by an iterative procedure, updating material parameters (C and m) by a gradient based optimization technique. The gradient of the objective function is computed by the finite differences method through the interaction between an external *python* script and the FE solver. This inverse procedure goes on until the objective function reaches a value under a prescribed threshold value [8].
In this kind of analysis the numerical model represents the *forward model* and the free inflation test is the experimental reference on which the inverse analysis is based [12]. Minimizing the error between results from the forward model and the experimental reference, accurate material parameters can be obtained.
On the other hand, inverse analysis can occasionally lead to solutions that are not physically valid, even the objective function is sufficiently small. Moreover, a limit of gradient based approaches, in spite of their fast convergence after few iteration steps, is the possibility to find a local minimum that gives a small value of the objective function but not represent the reality in the best way. Furthermore, a strong correlation between C and m exists, since either the variation of first or of the second parameter can lead to similar effect on the consistency of the material. This means that potentially infinite couples of C and m can give good results with

small values of the Q function, well predicting the behaviour of the material in the simulated test representing the experimental reference. Generally, if the solution is not sufficiently accurate, the obtained *C* and *m* values give good results in reproducing the test that has been used as experimental reference in the inverse analysis but give bad results when load conditions of the test change. Making the inverse analysis starts from values that are not far from real ones can bring to optimized results that can well represent the physical phenomenon. In this work material constants have been firstly calculated by the approach proposed by Enikeev and Kruglov and, then, they have been optimized through the described inverse analysis procedure and finally verified in different load conditions (changing the gas pressure in the free inflation test). In Fig. 4 results of the inverse analysis are shown. In order to compare the starting solution with the optimized one, the numerical dome height curve obtained with the starting *C* and *m* values achieved with the analytical approach has been illustrated in the same graph with the experimental and the optimized ones.

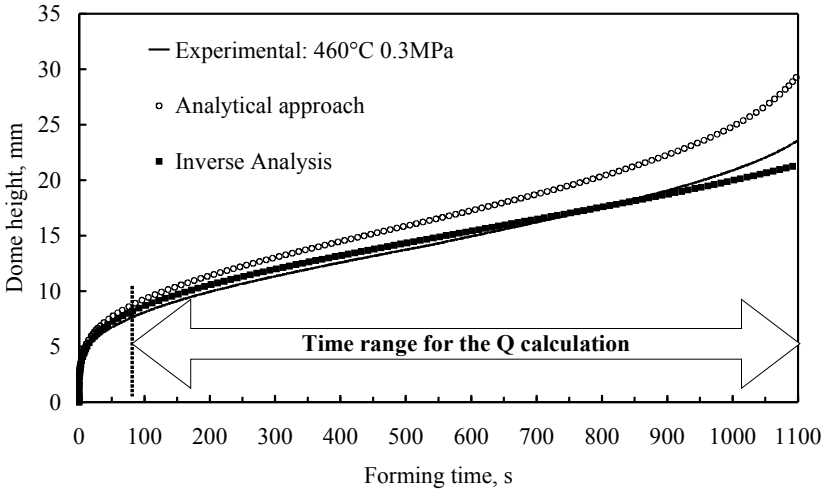

Figure 4. Inverse analysis: experimental dome height versus time curve compared with numerical ones before and after the inverse procedure.

For the experimental reference test (pressure: 0.3 MPa), in order to avoid numerical instabilities, the time range for the Q calculation was chosen excluding the initial and the final transient phases, during which the dome height rate rapidly changes (time range: 80 s ÷ 1100 s). After two iterations, the Q function is reduced from 0.021, corresponding to the starting value (obtained by the analytical approach), to 0.002 at the end of the optimization procedure. As can be seen in Fig. 4, the numerical curve obtained after the inverse analysis is much closer to the experimental one than the one obtained by the analytical approach. Material constants refined by the inverse analysis have been then verified simulating the test with a different pressure value (0.7 MPa) obtaining, also in this different load condition, a good agreement with experimental results.

4 PROCESS ANALYSIS

Free inflation tests can be considered a good way for the characterization of the material but are not enough complete to obtain information about the BF process and its potentialities and limits. In industrial applications of BF, the sheet strongly interacts with the die wall and with the die bottom to get the final shape. In this work the material characterization phase has been followed by an experimental and numerical analysis of the process in closed die forming tests. An experimental plan with constant pressure (CP) and different forming time values has been firstly carried out to observe the deformation evolution during the forming process. Then, a 3D numerical model of the closed die BF process has been created and calibrated on the basis of experimental results. The calibrated numerical model has been then used in a more direct

process analysis and for obtaining the pressure profile able to keep the strain rate in the sheet constant and close to a target value. The so calculated pressure profile has been then applied in experiments and differences, in terms of specimen characteristics after forming, between CP and constant strain rate (CSR) tests have been reported and discussed.

4.1 Constant pressure experimental tests

In the first phase of the experimental activity, CP tests have been carried out. Tests have been stopped at three different time instants to follow the material filling in die cavity. In particular, in Fig. 5, images of the specimens obtained with a CP of 0.7 MPa are shown for 300s, 900s and 1800s.

Figure 5. Constant pressure test with 0.7 MPa: formed specimens at three different forming time values (starting from the left 300s, 900s and 1800s).

From CP tests it is possible to note that, after 300 s, the sheet has already touched the die bottom and it has started the calibration phase to get to the final shape. After 900 s the contact area between the sheet and the die bottom has increased its extension and, especially along the median axis of the square section of the specimen, the sheet has touched the die vertical walls and gained a sharper corner radius. Finally, comparing specimens at 900 s and 1800 s, it can be said that the shape has no significant changes but along the diagonals the specimen have a more detailed profile.
The radius on the profile along the median axis of the square section has been measured by an optical digital system. In Fig. 6 the value of this geometrical parameter is plotted as a function of the forming time.

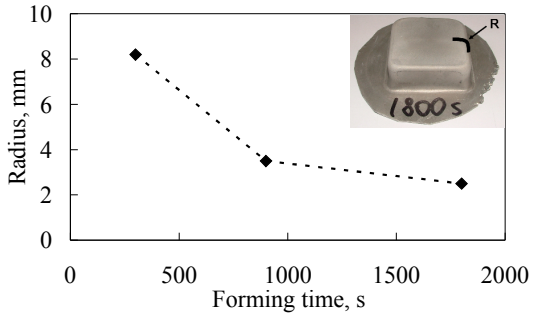

Figure 6. Specimen corner radius between the die cavity bottom and the die wall versus forming time.

The value of the radius rapidly decreases in the first part of the forming process: from 300 s to 900 s the radius value drops by 57% (from 8.2 mm to 3.2 mm) and takes other 900 s to reach a value of about 2.5 mm. It can be said that, at a CP of 0.7MPa, the die filling rapidly increases in the first part of the process, touching the die bottom in few seconds, but needs much longer forming time to get smaller values of the corner radii between the bottom and the wall of the specimen, especially along the diagonal axis of the square section of the specimen.

4.2 3D numerical model of the Blow Forming process

A 3D numerical FE model reproducing the forming process has been developed to test material constants also in closed die forming tests and to analyze in a more detailed way the BF process. In Fig. 7 a schematic representation of the FE model is shown.

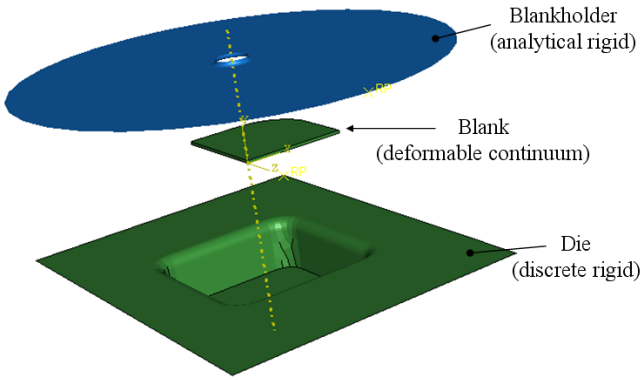

Figure 7. Schematic representation of the numerical 3D model of the BF process.

The die and the blankholder have been modelled as rigid surfaces. Only a quarter of the sheet has been modelled; continuum elements have been used and, in a similar way to the axial symmetric model, the sheet has been constrained in its periphery allowing only its thickness variation. Material behaviour has been modelled in the same way described in section 3.3 concerning the 2D model.

4.3 Model calibration

As seen also in experimental tests, the contact conditions between the sheet and the die surfaces strongly influences the process: after the contact between the sheet and the die bottom the filling rate suddenly decreases and the sheet takes a long time to get to the final shape. The sensitivity of the deformation process to the friction coefficient between the sheet and the die cavity surface is consequently high and by the numerical simulation it can be seen that different forming time and different thickness distribution can be obtained for different friction coefficients. Free inflation tests alone can't give sufficient information about contact conditions, since the contact area is relatively small, so the 3D numerical model of the closed die forming tests has been calibrated on the basis of the previous experimental tests with a prismatic die cavity. By an inverse analysis, similar to the one used to find material constants, the friction coefficient that better represent the real sheet behaviour has been searched among physically plausible values: a Coulomb friction coefficient close to 0.6 has been found. In Fig. 8 results, after the model calibration, are shown for the CP test at different forming times.

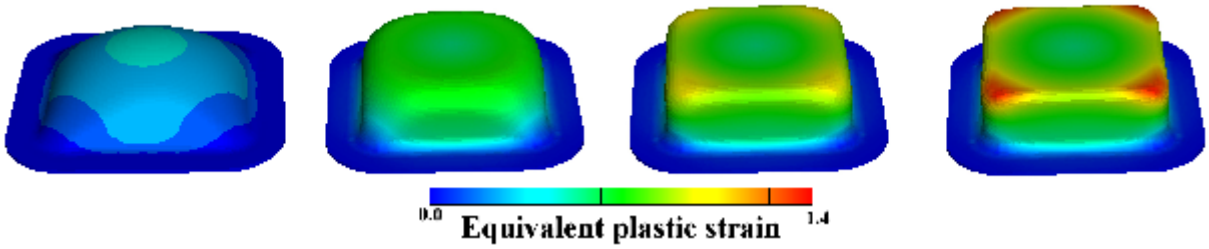

Figure 8. Numerical model of the closed die BF test: results after the model calibration for the a constant pressure test (0.7 MPa) at different forming times (60s, 300s, 900s, 1800s).

Numerical simulation allows examining the evolution of the forming process: before the contact between the sheet and the die cavity bottom, the most stressed area is in the central part of the specimen and the strain distribution is similar to the one of a free inflation tests; as soon as the sheet touches the die cavity bottom, the strain in the central zone of the specimen remain almost constant (denoting an almost instantaneous drop of the strain rate in this area) and the deformation moves to the edge areas; at the end of the forming process the areas of

the specimen along the diagonal axis appears to be the most critical where the highest thinning can be reported.

4.4 PRESSURE PROFILE FOR CONSTANT STRAIN RATE TEST

Once the material constants have been verified and the contact condition between die and sheet has been calibrated, the numerical model has been used to get the pressure profile able to get a CSR on the sheet during the process. Due to the geometry of the die cavity, sheet undergoes to different strain conditions according to the considered area and to the forming phase. Thus, significantly different strain rates can be found along the sheet and the location of critical zones changes during the process: in first phase, in which the sheet freely expand in the die cavity the most critical zone (with the highest strain rate value), is located on the dome apex, while in the second phase, after the sheet touches the die bottom, the highest strain rates can be found along the diagonal axis of the square section.
The ABAQUS software contains a built-in algorithm (named CREEP STRAIN RATE CONTROL) which allows the maximum strain rate, in a given set of elements, being controlled in order to have an almost constant value regulating the pressure load. This procedure gives good results even if, because of the step condition adopted, it changes the pressure load only if the strain rate value reaches an upper or a lower limit [11]. In this work it has been chosen an other algorithm based on the one proposed by [13]: the ABAQUS numerical model has been interfaced with a FORTRAN subroutine able to continuously control the pressure upon the sheet and to keep the maximum strain rate of the whole sheet around a constant value. The algorithm computes the optimal pressure by the following relation:

$$p(t+\Delta t)=\left[1-\ln\left(\frac{\dot{\varepsilon}_{comp}}{\dot{\varepsilon}_{target}}\right)\cdot\Delta t\right]\cdot p(t) \tag{4}$$

where p is the load value, $\dot{\varepsilon}_{comp}$ is the maximum equivalent strain rate value in the defined element set computed by the FE solver, $\dot{\varepsilon}_{target}$ is the target value of the equivalent strain rate, t is the analyzed time instant and Δt is the time increment, that has to be kept small to avoid oscillations in the pressure curve.
The algorithm implemented in the FORTRAN subroutine gives a more continuous curve and the equivalent strain rate is adequately kept constant around the target value. This kind of curve for the pressure controlling is also more suitable for the LabView program interfaced to the pressure regulator and for better results it can be approximated by a six order equation with an elevated correlation factor.
The chosen target strain rate was set on $5\text{x}10^{-4}$ 1/s; in Fig. 9 pressure profiles obtained both from the built-in ABAQUS algorithm and from the external subroutine are plotted.

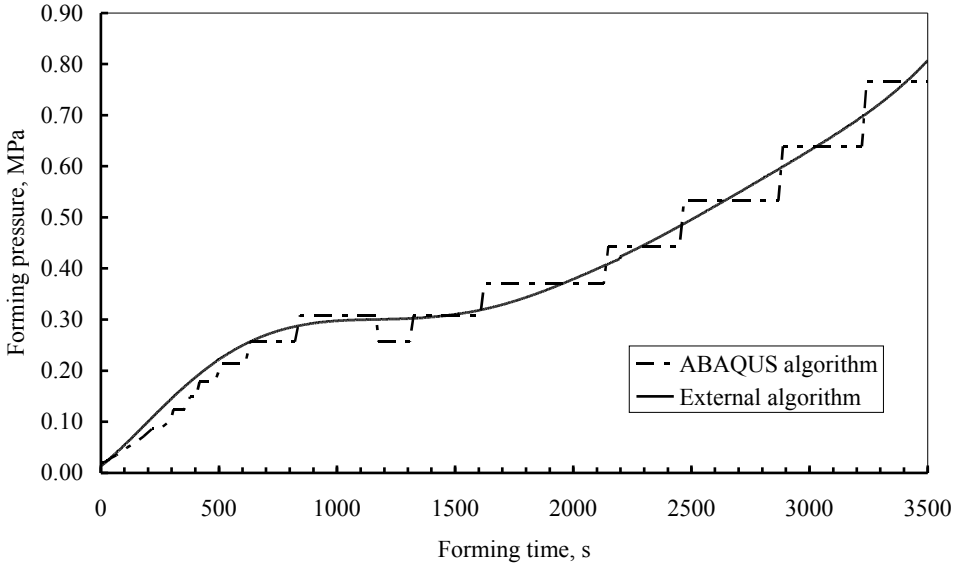

Figure 9. Constant strain rate closed die BF test: pressure profiles obtained both from the built-in ABAQUS algorithm and from the external subroutine.

The two different algorithms produces a similar trend of the pressure value: in the first phase, during which the most critical zone is in the centre of the specimen, before the contact between the sheet and the die bottom, the pressure increases with a decreasing derivative; in the second phase, during which the areas with the highest strain rate values are along the edges of the specimen, the pressure derivative is positive and rapidly raises. The pressure profile obtained from the external algorithm has been applied in a closed die forming test with the same material and the same cavity shape of previous tests. A forming time of 3500 s was chosen in order to get a die filling similar to the one achieved with a CP value of 0.7 MPa after 1800 s.

4.5 Constant pressure and constant strain rate comparison

Experimental test with CP have been compared with CSR ones to analyze the effectiveness of the optimized pressure profile adoption. First of all, experiments, as numerical simulations, show how, to get a similar die filling, the test with a CP value of 0.7 MPa takes about half the time needed with a CSR imposed on the sheet of $5x10^{-4}$ 1/s. In an industrial point of view time reduction can be a great advantage in the part manufacturing, but this advantage must go together with a good part quality. As mentioned before, post-forming characteristics is an important matter in SPF application and, in the specific of this work, optical microscopy, measurement of the thickness distribution and of the mechanical strength of the deformed material have been used as characterizing methodologies.

4.5.1 Thickness and microcavities comparison

One of the first comparisons has been done in terms of thickness distribution along the sheet: thickness values have been measured along the median axis of the square section of the formed specimens in both conditions (CP and CSR). Considering specimens with similar die filling, the corner radius zone corresponding to the area between the die wall and the die bottom is the most critical one in both cases; no significant differences can be found between the two different load conditions: the larger difference between the thickness in homologous measurement points in the two specimens is about 0.02 mm that is close to the precision of the measurement method.

Since thickness measurement has not denoted significant differences between the two specimens, the analysis has moved to the microcavities analysis by optical microscopy. In Fig.

10, two micrographs of the most critical zone along the diagonal corner of the formed part are shown.

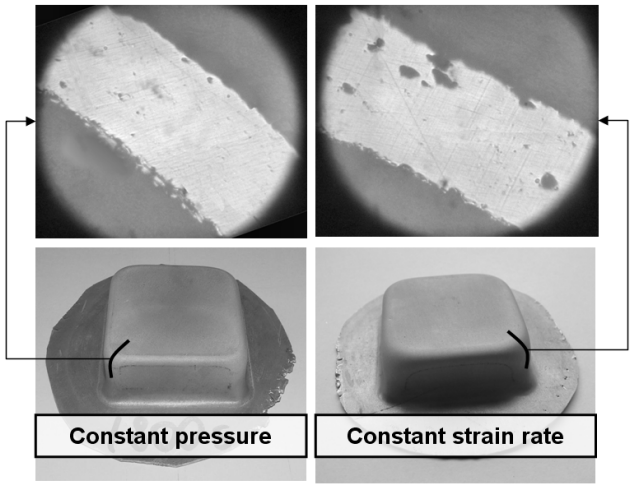

Figure 10. Micrographs of the most critical zone of the formed specimens for constant pressure (0.7MPa for 1800s) and constant strain rate ($5x10^{-4}$ 1/s for 3500s) with similar die filling.

Despite the pressure has been profiled in order to keep the strain rate around a controlled target value, a larger cavity presence in the specimen obtained by the CSR test can be seen. Cavity growth is related to the strain, to the strain rate that the material experiences in the forming process, to the grain size and to the temperature [14,15]. Since the temperature is the same, the strain level is almost the same in both specimens, the difference between them can be principally explained by the different strain rate and the different exposition times to elevate temperature that influences the grain size during the forming process.
Time dependencies of the cavity volume fraction have been evaluated analysing different time steps for the CP test: no significant time variation can be reported since cavities, in the central zone of the specimen, are evident even after 300 s. Their quantity and their dimension remain almost constant as far the CP test is concerned.

4.5.2 STRAIN RATE COMPARISON

To better understand the strain rate that the sheet experiences in the test with a CP, in Fig. 11 the variable is plotted versus time for two nodes of the FE mesh corresponding to the central area and to the diagonal corner. The central zone (point A in Fig. 11) is deformed with high strain rates in the first phase of the process, with a maximum value of about $1x10^{-2}$ 1/s, and after the contact between the sheet and the cavity bottom its strain does not change anymore. Analyzing the diagonal corner (point B in Fig. 11), after an initial peak the strain rate remains lower than $3x10^{-3}$ 1/s and continuously decreases till a value of $5x10^{-5}$ 1/s when the test is stopped (1800 s).

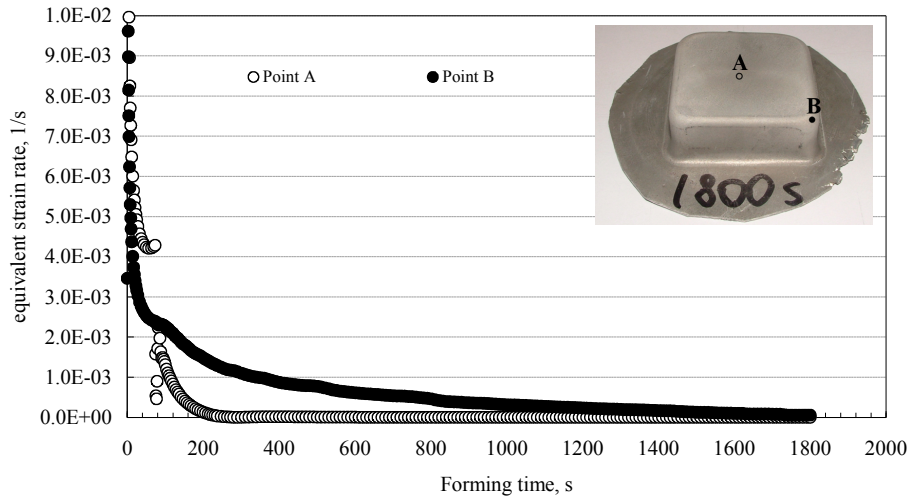

Figure 11. Strain rate versus time for two nodes of the FE mesh corresponding to the central area and to the diagonal corner in the constant pressure tests with a gas pressure of 0.7 MPa.

It can be stated that (i) the sheet, for the majority of the test duration, is not exposed to high strain rate values; (ii) the central part of the specimen experiences a strain rate higher than $4x10^{-3}$ 1/s for all the part of the test in which the sheet freely expand without touching the die bottom; (iii) in the second half the strain rate value become lower than the value that in the other test has been used as target value ($5x10^{-4}$ 1/s).

4.5.3 POST-FORMING MECHANICAL STRENGHT COMPARISON

Small tensile test specimens (gauge length 8 mm, width 5 mm) have been machined from the flat part of the formed component obtained from both CP and CSR tests. Tensile tests have been performed on the base material (undeformed) and on specimens obtained with CP and CSR. In Fig. 12 results are reported. In particular, for the CP tests, the material has been tests after three different forming times to understand the time influence on the mechanical strength of the material.

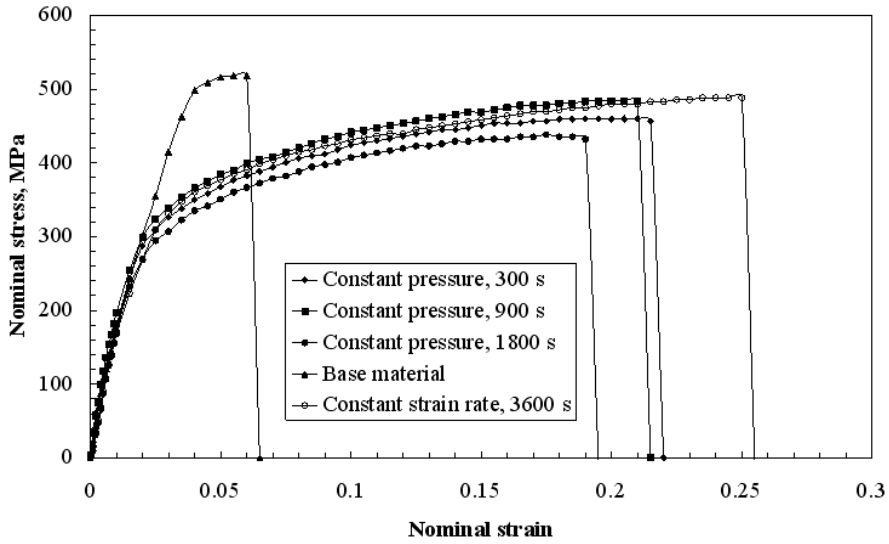

Figure 12. Tensile flow curves for the base material (before forming) and for formed specimens.

Both the ultimate tensile stress (UTS) and the yield stress of the material are negatively affected by the forming process. On the other hand, the material, that in the base conditions has a strong work hardening, gains ductility after the forming process. Moreover, ductility can

be considered one of the most significant factors in comparing tests with different load profiles. The UTS is, in fact, quite similar for all the specimens, its maximum value is registered for the CSR test, denoting a more sound post-formed material condition in the central area of the specimen. In the specimen formed with a CP ductility is always lower than the one of the specimen formed wit a CSR and inversely proportional to the forming time.
Another proof of the higher integrity of the material in the central part after the CSR test is the strain distribution in the tensile test specimen. By a digital image correlation system (ARAMIS 3D) the strain maps on the specimen can be obtained during the entire tensile test. For instance in Fig. 13, the major strain maps are plotted for tensile tests performed on specimens from the CP test (0.7 MPa and 1800 s) and the CSR test ($5x10^{-4}$ 1/s and 3500 s) that have achieved similar die filling.

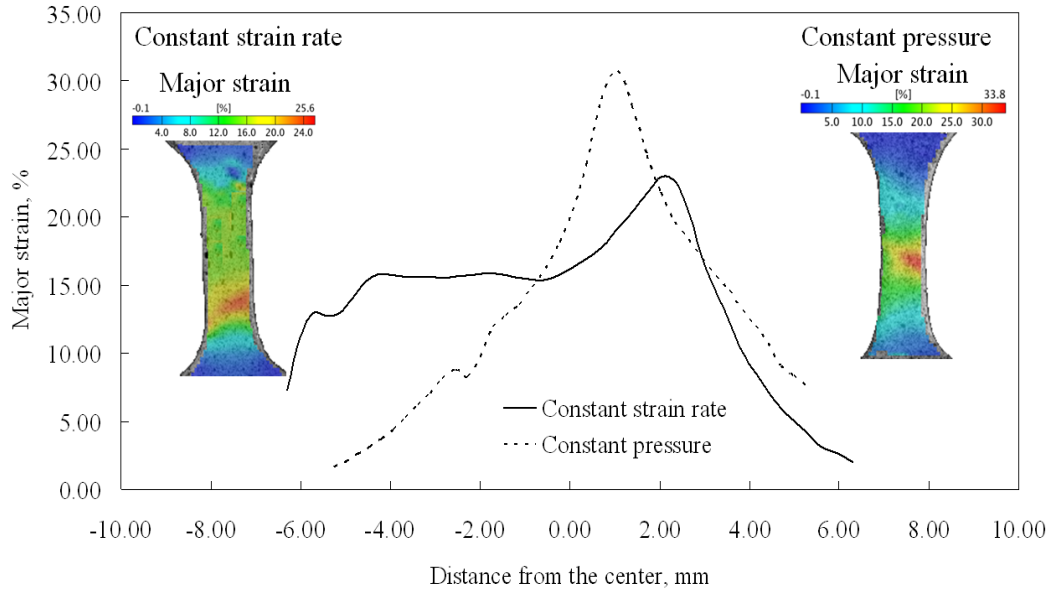

Figure 13. Major strain values for tensile tests performed on formed specimens from the CP test (0.7 MPa and 1800 s) and the CSR test ($5x10^{-4}$ 1/s and 3500 s) with similar die filling.

Analyzing local strain distribution, in the CSR test specimen a more uniform distribution can be found resulting in a global measured ductility higher than the one measured in the CP test, even if the maximum local strain value is higher in the latter one. This behaviour can be justified with a higher occurrence of defects in the material that has not been formed with a controlled strain rate.

5 CONCLUSIONS

The experimental-numerical methodology for the characterization of a SP material that have been proposed in this work, have been described and verified: testing the outputs of this methodology, in a BF process analysis, it can be seen that it represent a good instrument for the material characterization and for the process optimization. Numerical model can be used in predicting the material behaviour during forming and for optimizing the BF process according to the best material performances.
The experimental and numerical activities described and discussed in this work allow assessing that:

- material superplastic formability is strongly influenced by temperature and strain rate; in a free inflation test, changing the forming gas pressure and consequently the imposed strain rate, can lead to a great difference in the final dome height achieved before failure; in the explored range of pressure and temperature values and for the considered alloy, best results have been found for 460° C and low pressure values;

- for a datum temperature, material constants can be found by means of few bulge tests starting from an analytical approach and refining the solution by an inverse technique; based on a gradient based method, the described inverse procedure is fast and sufficiently accurate;
- in CP closed die BF test, strain rate strongly decreases after the contact between the sheet and the die cavity bottom.

Comparing a CP test with CSR test with similar die filling it can be said that:

- the test with a CP value of 0.7 MPa takes about half the time needed with a CSR imposed on the sheet of $5x10^{-4}$ 1/s;
- in the most critical zone (the corner area along the diagonal axis) lower cavities volume fraction can be observed for the CP test;
- the mechanical strength measured after forming in the central zone of the formed specimens, CSR shows a slightly higher UTS and a significantly higher ductility;
- in the CP test, cavities dimension and quantity reach their maximum value, in the central part of the formed specimen, in the first part of the test, during which the imposed strain rate is maximum.

A more detailed analysis can be done extending the explored temperature and pressure values to a wider range and verifying the proposed approach also for different values of those parameters. Free inflation tests, as well closed die forming tests, with a back pressure imposed on the sheet, can be carried out to reduce the cavitation phenomenon and to compare CP and CSR test in a different condition: reducing defects by cavitation, tests can be performed keeping constant the strain rate only in the area of the sheet that show maximum values of the strain in the final configuration and this, according to the part geometry, could speed up the process without reducing part quality.

6 Acknowledgements

Authors gratefully acknowledge the Alenia Aeronautica S.p.A. company and, in particular, Massimiliano Di Paola, for making the experiments possible and for the help given in the interpretation of results.

7 References

[1] R.M. Cleveland, A.K. Ghosh, J.R. Bradley, *Comparison of superplastic behavior in two 5083 aluminum alloys*. Materials Science and Engineering, 2003. A351, p. 228-236.

[2] N. Chandra, *Constitutive behaviour of superplastic materials*. International Journal of Non-Linear Mechanics, 2002. 37, p. 461-484.

[3] M.A. Nazzal, M.K. Khraisheh, *On the stability of superplastic biaxial stretching using finite element simulations*. 4th European Conference on Superplastic Forming Euro SPF'05, UK, Manchester, 2005.

[4] M. Bellet, E. Massoni, S. Boude, *Finite Element Modeling of Superplastic Sheet Forming Processes. Identification of Rheological and Tribological Parameters by Inverse Method*. Proceedings of NUMIFORM 2004, Ohio, Columbus, 2004.

[5] J.H. Cheng, *The determination of material parameters from superplastic inflation tests.* Journal of Materials processing Technology, 1996. 58, p. 233-246.

[6] M.K. Khraisheh, F.K. Abu-Farha, K.J. Weinmann, *Investigation of Post-Superplastic Forming Properties of AZ31 Magnesium Alloy*. CIRP Annals - Manufacturing Technology, 2007. 56, Issue: 1, p. 289-292.

[7] Z.P. Chen, P.F. Thomson, *A study of post-form static and fatigue properties of superplastic 7475-SPF and 5083-SPF aluminium alloys*. Journal of Materials Processing Technology, 2004. 148, Issue: 2, p. 204-219.

[8] D. Sorgente, G. Palumbo, L. Tricarico, *Material superplastic parameters valuation by a jump pressure blow forming test*. Key Engineering Materials, 2007. 344, p. 119-126.
[9] F. Jovane, *An approximate analysis of the superplastic forming of a thin circular diaphragm: theory and experiments*, International Journal of Mechanical Sciences, 1968. 10 p. 403-427.
[10]F.U. Enikeev, A.A. Kruglov, *An analysis of the superplastic forming of a thin circular diaphragm.* International Journal of Mechanical Sciences, 1995. 37, No. 5, p. 473-483.
[11]Abaqus Online Documentation: Version 6.7, 2007, Dassault Systèmes, 2007.
[12]G.R. Liu, X. Han, *Computational inverse techniques in nondestructive evaluation*. CRC Press, 2003.
[13]Y.M. Hwang , H.S. Lay, J.C. Huang, *Study on superplastic blow-forming of 8090 Al–Li sheets in an ellip-cylindrical closed-die*. International Journal of Machine Tools & Manufacture, 2002. 42, p. 1363–137.
[14]C.L. Chen, M.J. Tan, *Cavity growth and filament formation of superplastically deformed Al 7475 Alloy*. Materials Science and Engineering, 2001. A298, p. 235–244.
[15]J.J. Blandin, B. Hong, A. Varloteaux, M. Suery, G. L'Esperance, *Effect of the nature of grain boundary regions on cavitation of a superplastically deformed aluminium alloy.* Acta Materialia, 1996. 44, Issue: 6, p. 2317-2326.